The Dynamics of Idealized Convection Schemes and Their Effect on the Zonally Averaged Tropical Circulation

DARGAN M. W. FRIERSON

University of Chicago, Chicago, Illinois

ABSTRACT

In this paper, the effect of a simple convection scheme on the zonally averaged tropical general circulation is examined within an idealized moist GCM to obtain broad classifications of the influence of convection on the Tropics. This is accomplished with a simplified convection scheme in the style of Betts and Miller. The scheme is utilized in a moist GCM with simplified physical parameterizations (gray radiation, with zonally symmetric, slab mixed layer ocean boundary conditions).

Comparisons are made with simulations without a convection scheme [i.e., with large-scale condensation (LSC) only], with the moist convective adjustment (MCA) parameterization, and with various formulations and parameter sets with a simplified Betts–Miller (SBM) scheme. With the control run using the SBM scheme, the Tropics become quieter and less dependent on horizontal resolution as compared with the LSC or MCA simulations. The Hadley circulation mass transport is significantly reduced with the SBM scheme, as is the ITCZ precipitation. An important factor determining this behavior is the parameterization of shallow convection: without shallow convection, the convection scheme is largely ineffective at preventing convection from occurring at the grid scale.

The sensitivities to convection scheme parameters are also examined. The simulations are remarkably insensitive to the convective relaxation time, and only mildly sensitive to the relative humidity of the reference profile, provided significant large-scale condensation is not allowed to occur. The changes in the zonally averaged tropical circulation that occur in all the simulations are understood based on the convective criteria of the schemes and the gross moist stability of the atmosphere.

1. Introduction

Our picture of the Tropics is continually changing with the addition of new observations in this relatively data-sparse region. Many of these recent observations have provided compelling empirical tests for the theoretically based aspects of convection schemes, and the choice of parameters therein. For instance, the study of Brown and Bretherton (1997) demonstrates the correlation between boundary layer moist static energy and free tropospheric temperature, as postulated in the quasi-equilibrium (QE) hypothesis, used in many convection schemes. Zhang (2002, 2003), and Donner and Phillips (2003) examine the validity of the QE hypothesis using observations of convective available potential energy (CAPE). These studies indicate that while the QE hypothesis is not valid for short times, CAPE is in

QE for time scales of one day or longer. QE occurs at a shorter time scale in the west Pacific, where there is adequate availability of moisture for convection. The study of Bretherton et al. (2004) calculates the correlations between relative humidity and precipitation in the Tropics, and show that these quantities are indeed well correlated. However, they also find that implied convective relaxation times are larger than those typically used in models such as the Betts–Miller scheme; they find an approximate relaxation time scale of 12–16 h.

Motivated by these observational findings, and the desire to simulate the tropical general circulation with a scheme of maximum simplicity, we develop a simplification of the Betts–Miller convection scheme, and use this to study the zonally averaged climate of the Tropics within an idealized moist general circulation model (GCM). We focus primarily on the effect of convection on the Hadley circulation and the zonally averaged tropical precipitation distribution. Current general circulation models and their convection schemes typically

Corresponding author address: Dargan Frierson, University of Chicago, Chicago, IL 60637.
E-mail: frierson@geosci.uchicago.edu

have difficulty in simulating precipitation distributions within the intertropical convergence zone (ITCZ) and near the equator (Mechoso et al. 1995); in particular most GCMs have a tendency to form a double ITCZ that is not observed. There is relatively little theoretical understanding of the reasons for these deficiencies; this is, in part, because there has been relatively little study of the zonally averaged tropical circulation within models that bridge the gap between simple theories and full GCMs.

There are several notable examples of studies of the zonally averaged tropical circulation in idealized GCMs of full vertical resolution with moisture. For instance, Numaguti (1993) studies the tropical precipitation distribution and the Hadley circulation within an idealized moist GCM over an aquaplanet lower boundary. The author emphasizes the importance of the distribution of evaporation for the Hadley circulation and the large sensitivity of the precipitation to small changes in evaporation. He additionally finds that the convection scheme plays an important role in the determination of the Hadley circulation system. Hess et al. (1993) also find a large sensitivity to convection scheme in an aquaplanet GCM; this study along with Numaguti (1995) examines the sensitivity of the ITCZ location and strength to sea surface temperature (SST) distribution as well. The studies of Chao (2000) and Chao and Chen (2001, 2004) use an aquaplanet context, often with globally uniform SSTs, to study the effect of convective parameterization and other factors on creating a single or double ITCZ. They emphasize the competing roles of the Coriolis force and surface fluxes while finding that mass flux schemes are more likely to form a double ITCZ than moist convective adjustment (MCA).

From a different perspective, Satoh (1994) presents a theory for the moist Hadley circulation within an axisymmetric aquaplanet model with idealized parameterizations of moisture and radiation. His theory starts with energy balance in the subtropics, which are assumed to be dry. Balancing radiative cooling with adiabatic warming, and setting the lapse rate to the moist adiabat allows one to calculate subtropical subsidence rates. The subsidence then can be integrated to determine the strength of the cell. In this sense, convection does not strongly influence the zonally averaged circulation, as the control of the strength of the cell is limited to the subtropics where no convection occurs; his sensitivity tests confirm a lack of sensitivity to convective parameterization. However, this theory would not necessarily carry over into an atmosphere in which the subtropics are not completely dry, as clearly is the case in Earth's atmosphere. If precipitation can balance a significant fraction of the radiative cooling in the sub-

tropics, the Hadley circulation can be made weaker or stronger by changing the latent heating in this region. Our model provides a useful realm for the test of Satoh's theory in a model with axial eddies and a consistent energy balance and treatment of moisture.

a. Model framework

In Frierson et al. (2006) we have introduced a framework for idealized general circulation modeling which incorporates the dynamical effects of moisture in a simplified manner. The model integrates the full primitive equations on the sphere, with highly simplified physical parameterizations that facilitate comparison between full GCMs and simple theories. In this model, we use gray radiation, so radiative fluxes are a function of temperature alone (e.g., there are no cloud, or water vapor, radiative feedbacks). The boundary conditions are zonally symmetric aquaplanet (ocean covered) Earth, with a slab mixed layer ocean. In Frierson et al. (2006, 2007), we used large-scale condensation (LSC) only as the convection scheme. In those studies, we focused on the midlatitudes, and those results are robust for different convection schemes. However, the tropical circulation within this framework is sensitive to the choice of convection scheme. Storms with sizes of a few grid points dominate the Tropics in the LSC simulations.

To obtain a tropical climate in accordance with observations while retaining simplicity and a small number of parameters, we have designed a cumulus parameterization scheme in the style of Betts and Miller (Betts 1986; Betts and Miller 1986). This scheme and simplifications thereof are frequently used in simple or intermediate-complexity models (e.g., Neelin and Yu 1994; Yu and Neelin 1994, 1997; Neelin and Zeng 2000; Sobel et al. 2001; Frierson et al. 2004). Betts–Miller schemes assume that convection acts to relax humidity and temperature to equilibrium profiles with a specified relaxation time. In his review of cumulus parameterization, Arakawa (2004) emphasizes the relative insensitivity of GCMs to convection scheme because most schemes can be interpreted as performing a similar kind of relaxation toward moist adiabatic temperature profiles. On the other hand, some aspects of climate simulations are sensitive to even the most minute details of the convective parameterization. Simulations with the Geophysical Fluid Dynamics Laboratory (GFDL) version of the relaxed Arakawa–Schubert parameterization (Moorthi and Suarez 1992) in radiative–convective equilibrium indicate surprising sensitivity to such aspects of the scheme as entrainment limiters, cumulus momentum transport, and time step, among others (M. Zhao 2006, personal communication). Often these details of the scheme are not documented in publica-

tions; therefore, another goal of the development of the simplified Betts–Miller (SBM) scheme that we present here is to formulate a convection scheme that is easily reproducible by others while retaining fidelity to observations. Additionally, since the SBM scheme is not tied to any empirical parameters of the present climate, we hope that it can be useful for simulating a wide range of climates very different than our own.

b. Outline

We first present a complete description of the SBM scheme in section 2. We then study the dependence of the zonally averaged tropical circulation on the shallow convection parameterization in section 3. This section includes comparisons with LSC and MCA convection schemes and a study of resolution dependence. In section 4, we examine the sensitivity of the tropical climate to the SBM scheme parameters. We conclude in section 5.

2. Description of the SBM scheme

Betts–Miller convection schemes (Betts 1986; Betts and Miller 1986; Janjic 1994) take vertical profiles of temperature and humidity and calculate precipitation rates and changes in temperature and humidity by relaxing toward post-convective equilibrium profiles. This calculation is performed through several steps: calculating reference profiles; determining whether there will be deep, shallow, or no convection; relaxing toward the reference states; correcting to satisfy enthalpy conservation; and performing shallow convection. We describe how our schemes treat these situations. None of the discussion below depends on the choice of reference profiles of temperature and humidity (T_{ref} and q_{ref}, respectively); therefore, we describe this aspect of the scheme at the end of the section.

a. Convective criteria and first guess relaxation

Before determining the convective criteria, we relax the temperature and humidity in the following way:

$$\delta q = -\frac{q - q_{ref}}{\tau_{SBM}} \tag{1}$$

$$\delta T = -\frac{T - T_{ref}}{\tau_{SBM}}, \tag{2}$$

with τ_{SBM} the convective relaxation time, a parameter of the scheme. Then the precipitation due to drying and the precipitation due to warming, respectively, are

$$P_q = -\int_{p0}^{p_{LZB}} \delta q \, dp/g \tag{3}$$

$$P_T = \int_{p0}^{p_{LZB}} \frac{c_p}{L} \delta T \, dp/g, \tag{4}$$

where the integrals range from the surface to the level of zero buoyancy (LZB). The simplest criterion for deep convection is that both P_T and P_q are positive. The former being positive is equivalent to CAPE + CIN > 0 (with CIN the convective inhibition), if the reference temperature profile is a moist adiabat. The requirement $P_q > 0$ implies that there is more moisture in the column than in the reference profile. We now summarize different options that can be used under different regimes of P_T and P_q.

b. Deep convection: $P_T > 0$, $P_q > 0$

If both of the precipitation quantities P_T and P_q are positive, then we state that there is deep convection. However since these quantities will not be equal in general, we must devise a way to conserve enthalpy. The simplest way to accomplish this, also used by Betts (1986), is by changing the reference temperature by a uniform amount with height so that the changes in temperature (in enthalpy units) are opposite to the changes in humidity (in enthalpy units); that is, so $P_T = P_q$. The cooling that takes place in the lower troposphere when $P_q < P_T$ can be interpreted as roughly simulating the effect of downdrafts cooling at lower levels. An implication of the uniform change with height is that the reference profile is no longer an adiabat. This method of conserving enthalpy can be written as the following:

$$\Delta k = \frac{1}{\Delta p} \int_{p0}^{p_{LZB}} -(c_p T + Lq - c_p T_{ref} - Lq_{ref}) \, dp \tag{5}$$

$$T_{ref2} = T_{ref} - \frac{\Delta k}{c_p}, \tag{6}$$

where T_{ref2} is the corrected reference profile, which is then used in Eq. (2) to calculate temperature tendencies. When this method is utilized, the precipitation is solely dependent on the humidity relaxation, since the temperature is adjusted to match this. This allows for precipitation not to be simply proportional to CAPE. Because of the extreme sensitivity of CAPE to the properties of a small fraction of the column (the boundary layer; Donner and Phillips 2003), one might expect that a small enthalpy correction could break down correlations between CAPE and precipitation completely. Indeed, in the simulations presented in the next section, precipitation is slightly anticorrelated with CAPE.

c. Shallow convection: $P_T > 0$, $P_q < 0$

If the precipitation after the enthalpy conservation ends up being negative, we switch to the shallow convection scheme [if the enthalpy conservation scheme given in Eqs. (5)–(6) is used, this amounts to $P_T > 0$, $P_q < 0$]. To make this continuous in precipitation with the scheme that changes the temperature reference profile to conserve enthalpy, we make the net precipitation zero in this limit. We have constructed three methods to perform this adjustment, which we describe here and test in the next section.

The simplest option for shallow convection is not to adjust at all under these conditions (i.e., $\delta q = 0$, $\delta T = 0$). This introduces a certain amount of discontinuity when matched against any of the schemes for enthalpy conservation above, but this is the limit against which we test the other shallow convection schemes.

The first nontrivial shallow scheme that we propose is one that lowers the depth of shallow convection. This scheme finds the deepest height for which there is enough moisture for the precipitation to be identically equal to zero; that is, the integral in Eq. (3) above is zero. A height will exist for all cases where the boundary layer has enough moisture. The transition as the precipitation goes to zero will be continuous in all cases where the upper troposphere is being moistened. For the temperature relaxation, we also adjust within the lowered layer, changing the reference profile by a constant amount with height as calculated below to ensure enthalpy conservation. In this scheme, the parcels do not reach their level of zero buoyancy, so we are implicitly assuming some entrainment. This can be expressed as the following set of equations:

$$0 = \int_{p0}^{p_{\text{shall}}} \left(-\frac{q - q_{\text{ref}}}{\tau_{\text{SBM}}} \right) dp \tag{7}$$

$$\Delta k = \frac{1}{\Delta p} \int_{p0}^{p_{\text{shall}}} -(c_p T + Lq - c_p T_{\text{ref}} - Lq_{\text{ref}}) \, dp \tag{8}$$

$$T_{\text{ref2}} = T_{\text{ref}} - \frac{\Delta k}{c_p}, \quad p_{\text{shall}} < p < p_0, \tag{9}$$

where p_{shall} is selected to satisfy Eq. (7). Equations (1) and (2) (with T_{ref2} used in the latter) are then used in the range $p_{\text{shall}} < p < p_0$ to calculate humidity and temperature tendencies. We refer to this method as the shallower shallow convection scheme.

Another scheme that we propose involves changing the reference profiles for both temperature and humidity so the precipitation is zero. This scheme does not change the depth of shallow convection, and instead simply changes the reference profile of humidity by a uniform fraction with height all the way up to the level of zero buoyancy, to make the precipitation zero. The temperature reference profile is changed in the usual manner, adjusting by a uniform amount with height so that its predicted precipitation is zero. This scheme can be written as

$$\Delta q = \int_{p0}^{p_{\text{LZB}}} (q - q_{\text{ref}}) \, dp \tag{10}$$

$$Q_{\text{ref}} = \int_{p0}^{p_{\text{LZB}}} (-q_{\text{ref}}) \, dp \tag{11}$$

$$f_q = 1 - \frac{\Delta q}{Q_{\text{ref}}} \tag{12}$$

$$q_{\text{ref2}} = f_q q_{\text{ref}} \tag{13}$$

$$\Delta T = \frac{1}{\Delta p} \int_{p0}^{p_{\text{LZB}}} -(T - T_{\text{ref}}) \, dp \tag{14}$$

$$T_{\text{ref2}} = T_{\text{ref}} - \Delta T. \tag{15}$$

Equations (1) and (2), using the adjusted reference profiles q_{ref2} and T_{ref2}, then give the tendencies for humidity and temperature. We call this the qref shallow convection scheme because the humidity profile is adjusted.

d. Reference profiles

For our temperature reference profile, we use the virtual pseudoadiabat for our temperature profile, meaning water vapor of the parcel and the environment are taken into account in the calculation of buoyancy, but the condensate immediately falls out. For the humidity profile, we specify a fixed relative humidity relative to this calculated reference temperature structure; this is the method utilized by Neelin and Yu (1994). This introduces the second parameter of the scheme. Adjustment occurs from the surface to the level of zero buoyancy of a parcel lifted from the lowest model level.

3. Sensitivity to shallow convection scheme

a. Model setup

A full description of the model is given in Frierson et al. (2006). To summarize, the model integrates the primitive equations using the spectral method, and fourth-order hyperdiffusion. The lower boundary is a slab mixed layer surface with vertically integrated heat capacity 10^7 J K^{-1} m^{-2}. There are no ocean heat transports, and no sea ice. The radiation scheme is gray ra-

diative transfer, so water vapor and other constituents have no effect on radiative transfer. The longwave optical depths of the gray scheme are designed to approximate the distribution of water vapor in today's climate. The net solar flux at the top of the atmosphere is tuned to the annual mean net top of atmosphere shortwave flux, with no seasonal or diurnal cycle. Surface fluxes are calculated with a drag law with drag coefficients calculated as a function of the height of the lowest level and the surface Richardson number, and equal roughness lengths for momentum, temperature, and humidity. Boundary layer diffusive fluxes are calculated with a K-profile scheme up to a prognostic boundary layer depth, defined as the lowest height at which a critical bulk Richardson number is exceeded. Saturation specific humidities are calculated with an analytic Clausius–Clapeyron expression.

Here our model setup is identical to Frierson et al. (2006) with the addition of the convection scheme and one additional change. To obtain a more realistic energy balance at the surface and strength of the hydrologic cycle, we specify a solar heating within the atmosphere. This is calculated by specifying optical depths for shortwave radiation τ_S within the atmosphere. Then we solve

$$\frac{dD_S}{d\tau_S} = -D_S \qquad (16)$$

with boundary condition $D_S(\tau_S = 0) = R_s$ [the top-of-atmosphere (TOA) solar radiation], and

$$Q_S = \frac{1}{c_p\rho}\frac{\partial D_S}{\partial z}. \qquad (17)$$

The latter is applied as a source term in the temperature equation. Optical depths are specified as

$$\tau_S = \tau_{S0}\left(\frac{p}{p_0}\right)^4. \qquad (18)$$

The parameter τ_{S0} is set to a value of 0.2, which implies that 18% of the TOA shortwave radiation is absorbed within the atmosphere. We then specify an albedo of 0.38 at the surface for all latitudes, which ensures that 51% of R_s is absorbed at the surface, and 31% of R_s is reflected to space. This provides an energy balance and hydrologic cycle strength that is more in accordance with observations.

The simulations below, unless otherwise noted, are run at T42 resolution with 25 vertical levels (spaced the same as in Frierson et al. 2006). We integrate for 1800 days, with the last 1440 days used for averaging. Time means are calculated using averages over each model time step, and spectra are calculated using instanta-neous values sampled once per day. The control simulation with the SBM scheme uses the shallower shallow convection scheme, and has the SBM parameters $\tau_{SBM} = 2$ h and $RH_{SBM} = 0.7$.

b. Comparison with LSC and MCA simulations, and with different shallow convection schemes

We begin by examining snapshots of precipitation for a simulation with LSC only, and the SBM scheme with the shallower scheme, the qref scheme, and no shallow convection scheme, shown in Fig. 1. The LSC simulations have large amounts of precipitation at small scales, a few grid points in size. Much of the Tropics and subtropics are without precipitation at any given instance, although tropical storm–like disturbances can be seen propagating sparsely throughout the subtropics and into midlatitudes. Simulations with MCA (not shown) are qualitatively indistinguishable from the LSC snapshot. When the SBM scheme is used but is integrated without a shallow convection scheme, the snapshot resembles the LSC case to a large extent, with slightly less concentrated precipitation events. In contrast, when either the shallower or the qref shallow convection schemes are used, tropical precipitation ceases to occur at small scales only, and is instead concentrated in more diffuse, zonally oriented bands. A larger fraction of the Tropics and subtropics is precipitating at any time in these simulations, but there remain dry regions in much of the subtropics and some of the deep Tropics. Tropical storms again propagate in the subtropics, but these are less prominent than in the LSC simulations. The shallower and qref simulations are nearly indistinguishable in Fig. 1, with tropical precipitation occurring at a slightly smaller scale when the shallower scheme is used.

As a more quantitative examination of typical sizes of convection in the Tropics, we plot the spectrum for the vertical velocity $\omega = (Dp/Dt)$ at the equator at 560 hPa in these simulations, presented in Fig. 2. The MCA and LSC simulations have the most variance of ω, with the SBM with no shallow convection intermediate, and the two simulations with shallow convection last. There is a clear spectral peak at wavenumber 2 for the shallower and qref SBM simulations, implying large-scale organization of convection in these cases. The shallower simulation has slightly more variance at smaller scales as compared with qref. In contrast, for the LSC, MCA, and SBM with no shallow convection cases, the spectrum is much less peaked, and significant power exists out to small scales. Much of the spectrum occurs near the grid scale for these simulations, suggesting there will be some sensitivity to horizontal resolution (which we analyze in more detail in section 3d). The
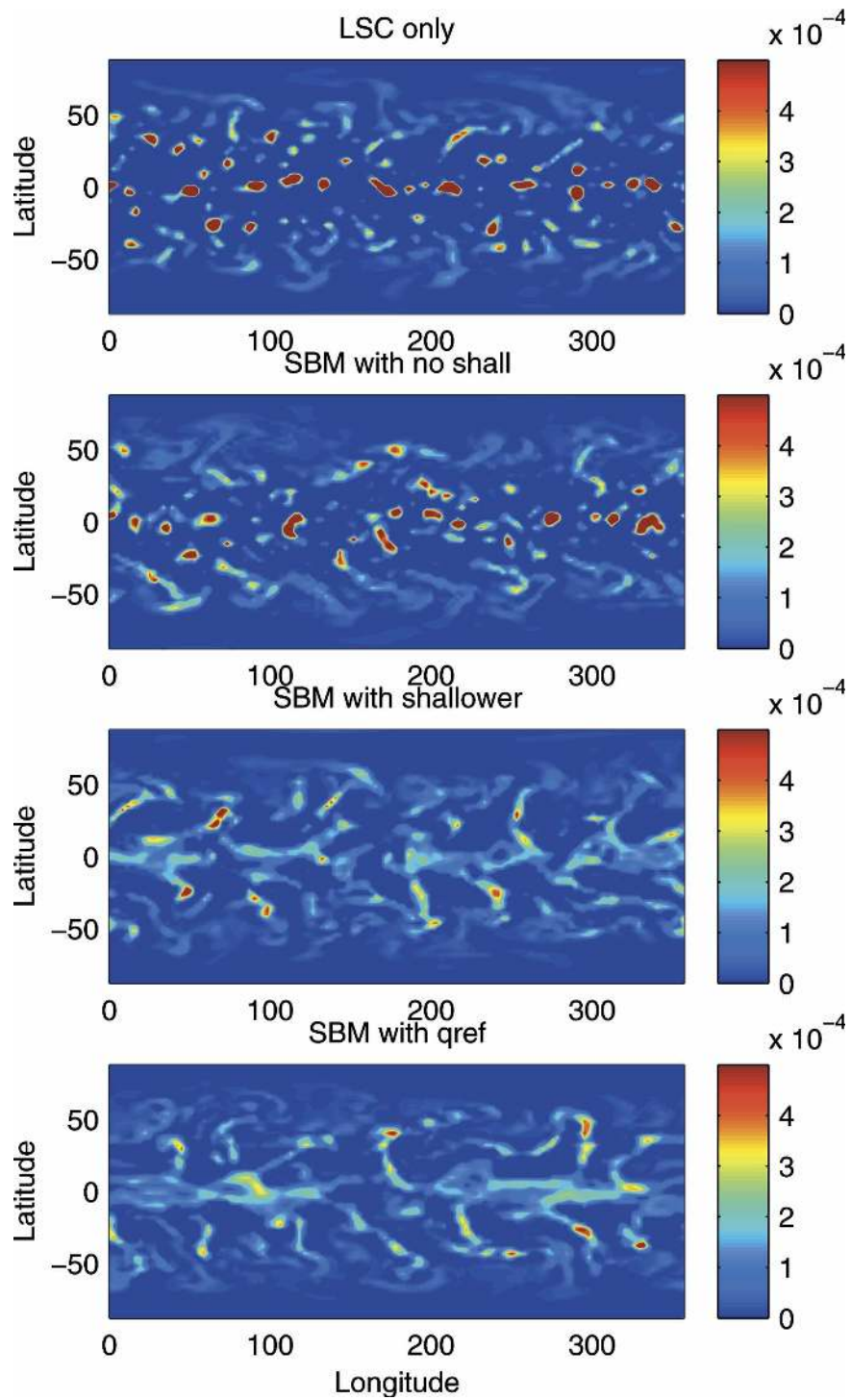
FIG. 1. Instantaneous precipitation (at the last time step of simulation) for (top)–(bottom) LSC only, the SBM scheme with no shallow convection scheme, the SBM scheme with the shallower shallow convection scheme, and the SBM scheme with the qref shallow convection scheme.
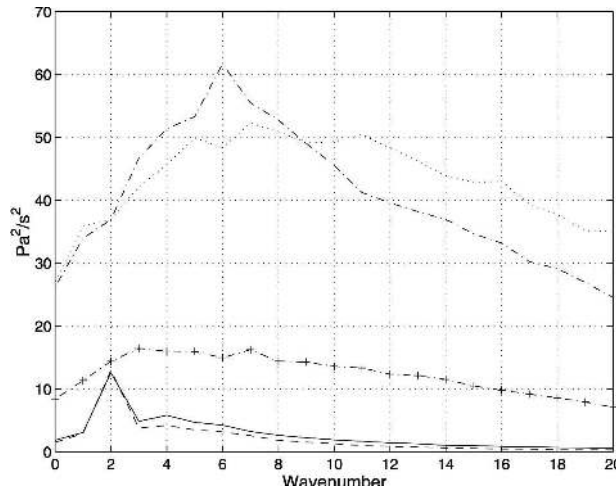
FIG. 2. Spectrum for vertical velocity (ω) at 560 hPa for the control SBM scheme with the shallower shallow convection scheme (solid), the SBM scheme with qref (dashed), the SBM scheme with no shallow convection (dashed–dotted with + symbols), the LSC only simulation (dotted), and MCA (dashed–dotted).
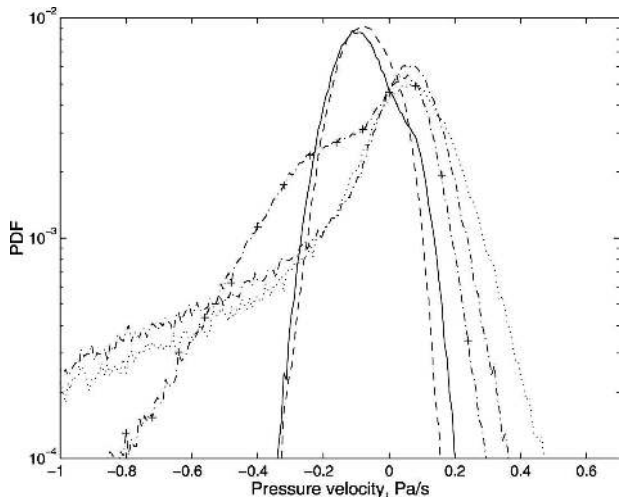

FIG. 3. Probability density function for vertical velocity (ω) at 560 hPa at the equator for the control SBM scheme with the shallower shallow convection scheme (solid), the SBM scheme with qref (dashed), the SBM scheme with no shallow convection (dashed–dotted with + symbols), the LSC only simulation (dotted), and MCA (dashed–dotted).

presence of gridscale precipitation is not surprising in the schemes with an abrupt convective criterion; that is, LSC and MCA, which require saturation of a grid box for convection to occur. The abrupt criterion leads to build-up and rapid release (upon saturation) of convective instability, which has peak growth rates at the smallest scale (see, e.g., Garner et al. 2007). Evidently, without the use of shallow convection, the relaxed adjustment of the SBM scheme is unable to prevent build-up and rapid release of instability, and hence the occurrence of convection at scales near the grid scale.

In Fig. 3, we plot the probability density function (PDF) for ω at the equator at 560 hPa for the same simulations. The SBM schemes with shallow convection exhibit more steady upward motion, with few extreme events. There is a single peak in the PDFs in these two cases that falls off relatively symmetrically on either side, especially in the qref case. The LSC and MCA cases, on the other hand, exhibit a peak in the PDF over weak downward motion, but with significantly more prevalent extreme events. While updrafts within the Tropics do occupy a small fractional area as compared with downdrafts, one should be careful in relating this plot to such observations since the GCM PDFs represent vertical motion averaged over a 2.8° area. The SBM with no shallow convection has a similar peak as the LSC and MCA cases, but fewer extreme events on both the downdraft and the updraft side.

We next examine properties of the zonally averaged circulation for these simulations, starting with the sea surface temperatures for reference in Fig. 4. There are

several notable differences with observations: these include the increased equatorial SSTs, especially prevalent in the cases with shallow convection, which occurs because of the reduced wind speeds in those locations. The SSTs are less flat than observations in all cases as well, which is due to the lack of ocean heat transport in the model. The results presented here are not sensitive to the depth (vertically integrated heat capacity) of the oceanic mixed layer. This indicates that the temporal
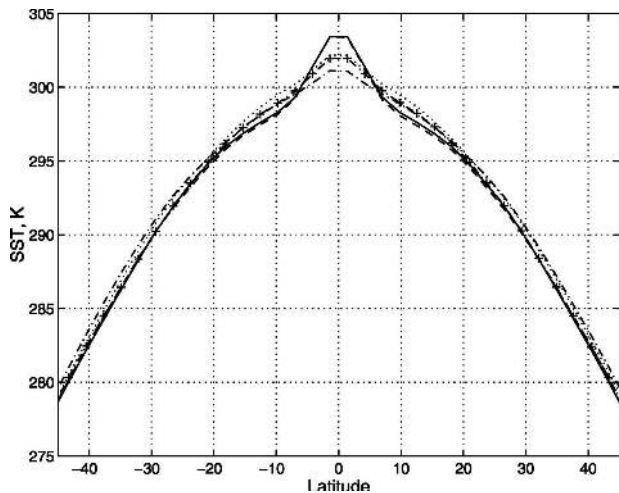

FIG. 4. SST (K) for the control SBM scheme with the shallower shallow convection scheme (solid), the SBM scheme with qref (dashed), the SBM scheme with no shallow convection (dashed–dotted with + symbols), LSC only (dotted), and MCA (dashed–dotted).
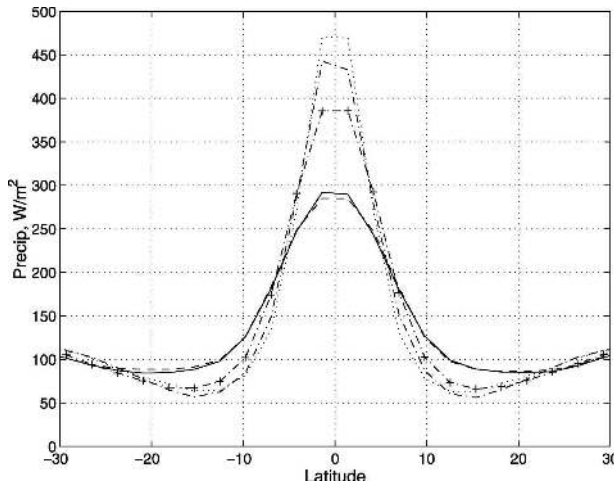
FIG. 5. Precipitation (W m^{-2}) for the control SBM scheme with the shallower shallow convection scheme (solid), the SBM scheme with qref (dashed), the SBM scheme with no shallow convection (dashed–dotted with + symbols), LSC only (dotted), and MCA (dashed–dotted).

variability of the SSTs (which can be made large by decreasing the depth, or essentially zero by increasing the depth) is not important in determining the zonally averaged circulation in this model. Further, the results here are not sensitive to the different SST distributions in Fig. 4: running the cases with different convection schemes over the same fixed SST distributions leads to similar properties of the convective organization, and enhanced differences in the Hadley circulation system between the SBM and LSC/MCA cases when compared with the mixed layer cases we present here.

To evaluate the effect of shallow convection on the Hadley circulation system, we first plot the precipitation distribution for the different simulations in Fig. 5. Each of these simulations exhibits a single maximum at the grid point closest to the equator, and a local minimum in the subtropics; however, the values of the respective maxima and minima vary greatly with convection scheme. In the two simulations with shallow convection, the precipitation at the equator is significantly decreased and the subtropical precipitation is enhanced compared with the other simulations. The agreement between these two SBM schemes with shallow convection is remarkable. The MCA and LSC simulations, on the other hand, have approximately 50% larger equatorial precipitation, and an approximately 35% smaller minimum in the subtropics. The SBM scheme with no shallow convection differs significantly from its SBM counterparts with shallow convection; it lies somewhat intermediate between these and the LSC and MCA cases. The mean tropical precipitation (averaged equatorward of 30°) changes by less than 4% in all these five

TABLE 1. Precipitation at the equator (W m^{-2}) and maximum meridional overturning streamfunction (10^9 kg s^{-1}) for the simulations varying convection scheme and shallow convection scheme.

Simulation	P(eq)	max(Had)
SBM w/shallower	291	184
SBM w/qref	285	183
SBM w/no shallow	386	250
LSC	438	277
MCA	470	273

simulations: the changes in precipitation are essentially a redistribution between the ITCZ and the subtropics.

The increased precipitation for the LSC and MCA cases is associated with an increase in the Hadley circulation, which converges moisture toward the equator. The maximum meridional overturning streamfunction values for the simulations (in 10^9 kg s^{-1}) are given in Table 1, along with the precipitation values at the grid boxes closest to the equator (in W m^{-2}); these are roughly proportional. The Hadley circulation is stronger than observations in all cases, a fact we understand from the lack of ocean heat transport in the simulations (either explicit, or implied from fixed SST boundary conditions). We discuss reasons for the differences in Hadley circulation and equatorial precipitation among these five cases in section 3c.

We next study the energy transports by the Hadley circulation, plotting the meridional moist static energy flux by the mean flow, $\int_0^{p_s} \overline{v}\,\overline{m}\,dp/g$, with $m = c_p T + gz + Lq$, for the different shallow schemes in Fig. 6.
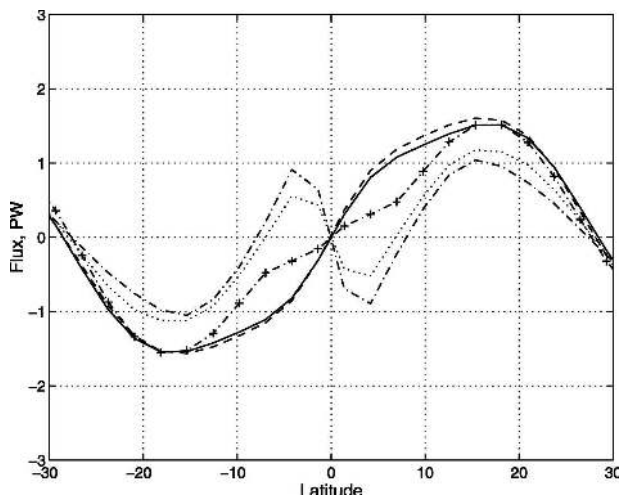

FIG. 6. Vertically integrated meridional moist static energy flux by the mean flow for the control SBM scheme with the shallower shallow convection scheme (solid), the SBM scheme with qref (dashed), the SBM scheme with no shallow convection (dashed–dotted with + symbols), LSC only (dotted), and MCA (dashed–dotted).

Surprisingly, the Hadley circulations in the LSC only and MCA simulations flux energy toward the equator in the deep Tropics. However, this equatorward transport is offset by strong eddy fluxes of moisture in this region, ensuring that the total energy transport is poleward at all latitudes in all cases. In fact, the total energy transports for these simulations have comparatively small differences in all cases (implying the outgoing longwave radiation, and the meridional temperature profiles are similar in all cases). Both of the SBM schemes with shallow convection give similar Hadley cell fluxes, with poleward fluxes at all latitudes within the Hadley cell, and achieving maxima of approximately 1.5–1.6 PW at latitudes between 15° and 19°. The SBM scheme with no shallow convection has reduced energy fluxes within the deep Tropics, but never becomes equatorward. The profile essentially matches onto the other SBM scheme fluxes poleward of the maximum flux. The LSC only and MCA simulations achieve significantly less poleward transport by the mean flow in general.

Despite a 50% stronger Hadley circulation, the LSC and MCA simulations transport significantly less energy poleward. The appropriate quantity to consider here is the gross moist stability (Neelin and Held 1987), which we define here as the amount of energy transported per unit mass transport:

$$\Delta m = \frac{\int_0^{p_s} \bar{v}\bar{m}\, dp}{\int_{p_m}^{p_s} \bar{v}\, dp}, \qquad (19)$$

where Δm is the gross moist stability, m is the moist static energy, p_s is the surface pressure, and p_m is some midtropospheric level (defined so that the equatorward mass flux occurs mostly below this level, and the poleward mass flux occurs above). This quantity is plotted for the SBM case with shallower shallow convection, the SBM case with no shallow convection, and the LSC only case in Fig. 7. The gross moist stability for all cases increases sharply away from the equator to the edge of the Hadley circulation where this quantity becomes ill defined. However, the values at the equator are significantly different for the three cases: approximately 6, 2, and −6 K for the SBM with shallower shallow convection, SBM with no shallow convection, and LSC only, respectively.

c. Interpretation of the Hadley cell changes

We now offer two explanations for the large change in Hadley circulation (and thus the ITCZ precipitation
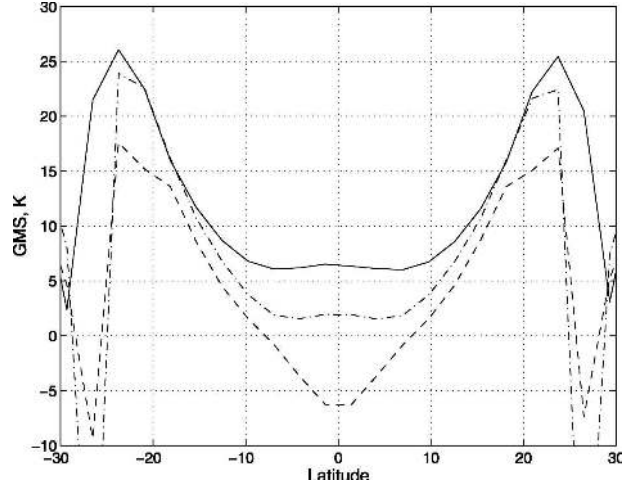

FIG. 7. Gross moist stability for the control SBM scheme with the shallower shallow convection scheme (solid), the SBM scheme with no shallow convection (dashed–dotted), and LSC only (dashed).

since this roughly scales with the circulation strength) with the different convection schemes. These two theories are somewhat linked: both relate the changes in the strength of the overturning to the abruptness of the convective criteria.

A first interpretation of the circulation changes involves the determination of the gross moist stabilities of the simulations (Fig. 7). In standard Hadley cell theories (e.g., Held and Hou 1980), the stability of the atmosphere is key in determining the strength of the circulation. In the SBM with shallower simulation, the gross moist stability is large enough at all latitudes that the mean flow can transport enough energy poleward to flatten temperatures with a modest strength Hadley circulation; the convection scheme has provided a stabilizing influence over the deep Tropics. In the LSC only case, on the other hand, the gross moist stability is smaller on average, so it is plausible that this means a stronger Hadley circulation is needed to produce flat temperatures. In the region where the gross moist stability is negative, even an extremely strong Hadley circulation cannot produce energy fluxes sufficient to flatten tropical temperatures: here small-scale eddies flux large amounts of latent heat poleward to keep the temperatures flat. It is likely that both the eddy moisture fluxes and the gross moist stability reduction are important in determining the Hadley circulation strength in the LSC only and MCA cases.

The gross moist stability can be thought of as the difference in moist static energy in upper tropospheric convective outflow regions minus the moist static energy in the lower tropospheric or boundary layer inflow regions. The gross moist stability increase in the control

SBM case is due to the penetrative nature of the convection scheme in this case, which increases the typical depths of convection and outflow moist static energy. In the LSC and MCA cases, the convective criterion is more difficult to satisfy (saturation is required for convection), and convection tends to occur in bursts. Within these bursts, convective depths are often less, which causes the gross moist stability to be reduced in these cases. In the SBM simulations with no shallow convection, the gross moist stability is less because shallow convection drains moisture from the boundary layer and deposits it into the free troposphere, causing less moist static energy in the lower troposphere and increasing the stability as well.

In the LSC only global nonhydrostatic simulations of Garner et al. (2007), which use the same physics package as this model, the gross moist stability of the atmosphere increases when the typical sizes of convective plumes are made artificially larger by performing a hypohydrostatic transformation to the vertical momentum equation. The increase in gross moist stability in this case is due to increases in the depth of convection as well, this time because there is less entrainment of dry environmental air into the wider convective plumes.

The second interpretation of the increased Hadley circulation invokes the energy budget in the subtropics. This region of subsidence from the Hadley circulation is significantly less humid than the surrounding regions. In the cases with more difficult convective criteria to satisfy (e.g., the LSC or MCA cases that require saturation to precipitate), there is therefore much less precipitation in the subtropics. In the SBM cases with shallow convection, by contrast, it is easier to convect in this region. For instance, the precipitation at $15°$ degrees is 90 W m^{-2} in the shallower SBM case, compared with 57 W m^{-2} in the LSC only case. In the SBM cases with shallow convection, this increased precipitation can counteract more of the radiative cooling in the thermodynamic equation in the subtropics (the radiative cooling changes little from case to case). With approximately the same lapse rate, less subsidence is then required to balance thermodynamically, creating a weaker Hadley circulation. This thermodynamic balance argument is complicated somewhat by eddy dry static energy fluxes; however, these remain small out to approximately $15°$, and change little from case to case outside of this region. The SBM case with no shallow convection is intermediate between the LSC only and SBM with shallow convection cases, because shallow convection helps to propagate moisture from the boundary layer and the free troposphere, and thus increases the ease of subtropical convection.
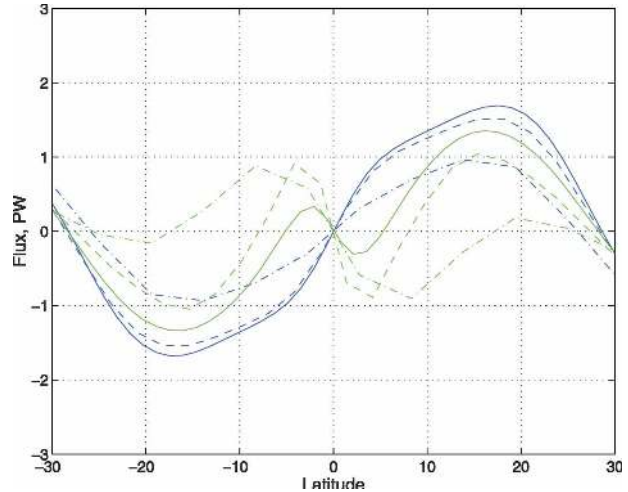

FIG. 8. Vertically integrated meridional moist static energy flux by the mean flow for the control SBM scheme (blue lines) and the LSC only simulations (green lines) at T85 (solid), T42 (dashed), and T21 (dashed–dotted).

d. Sensitivity to horizontal resolution

We now investigate sensitivity to horizontal resolution in the LSC only case and the control SBM case (with shallower shallow convection) by comparing with simulations at T21 and T85 resolution, all with 25 vertical levels. Since the precipitation is concentrated near the grid scale in the LSC only case, one might expect a greater sensitivity to resolution in this case. We first examine the vertically integrated meridional moist static energy transport by the mean flow, plotted in Fig. 8. The LSC only case shows significant change with resolution up to T85 [Frierson et al. (2006) found that similar simulations at T85 resolution were essentially converged as compared to T170]. The region of equatorward transport by the mean flow in the LSC cases is balanced by strong poleward eddy moisture fluxes, which cause the net moist static energy transport (mean + eddy) to be similar in all cases. The equatorward transport by the mean flow decreases with resolution, as do the eddy moisture fluxes. In contrast, the SBM scheme exhibits only minor change in resolution from T42 to T85 (although the T21 case is unresolved). The SBM convection scheme with shallow convection provides significantly improved convergence with resolution within the Tropics for this field. The equatorial precipitation and maximum Hadley circulation transport are given in Table 2. These fields both exhibit some dependence on resolution for the LSC simulations as well as the SBM scheme up to resolutions of T85. The SBM scheme is better converged at T21 resolution than the LSC simulations, but this resolution is

TABLE 2. Precipitation at the equator (W m^{-2}) and maximum meridional overturning streamfunction (10^9 kg s^{-1}) for the simulations varying resolution.

Simulation	P(eq)	max(Had)
SBM, T85	314	197
SBM, T42	291	184
SBM, T21	193	124
LSC, T85	482	268
LSC, T42	438	277
LSC, T21	214	137

still insufficient to obtain a proper Hadley circulation or precipitation distribution.

We now consider the resolution dependence of the zonal wind, plotted in Fig. 9 for the control SBM simulations and Fig. 10 for the LSC only simulations. At T21 resolution, both simulations exhibit significant equatorial superrotation (westerly zonal winds at the equator) in the upper troposphere. Surface zonal wind profiles are much more diffuse at T21 with both schemes as well, attaining minima of only -3.1 and -5.7 m s^{-1} for the LSC only case and SBM case, respectively, as compared to -8.5 and -9.7 m s^{-1}, respectively, at T85. With the SBM scheme, the superrotation is eliminated at T42 resolution, and the profile at T85 is essentially identical to the T42 simulation. By contrast, with the LSC only simulation superrotation weakens as resolution is increased, but remains even at T85. Similar simulations in Frierson et al. (2006) have equatorial superrotation eliminated at T170 resolution, but existing at resolutions below this. The full GCM study of Manabe et al. (1970), which uses the MCA parameterization, also shows superrotation at low resolution, disappearing at high resolution.

These results give us confidence that tropical circulations with the SBM can be adequately studied at horizontal resolutions of T42. However, resolutions of T21 appear to be inadequate to reproduce most aspects of tropical climate. Without a convection scheme, a higher resolution (of T85 or higher) is required to obtain convergence of some tropical climatic variables such as zonal winds or Hadley cell energy transports.

4. Sensitivity to SBM parameters

a. Sensitivity to τ_{SBM}

The SBM scheme has only two parameters after the choice of shallow convection scheme: τ_{SBM} and RH$_{SBM}$. We first examine sensitivity to the relaxation time τ_{SBM} with RH$_{SBM}$ = 0.7 and the shallower shallow convec-
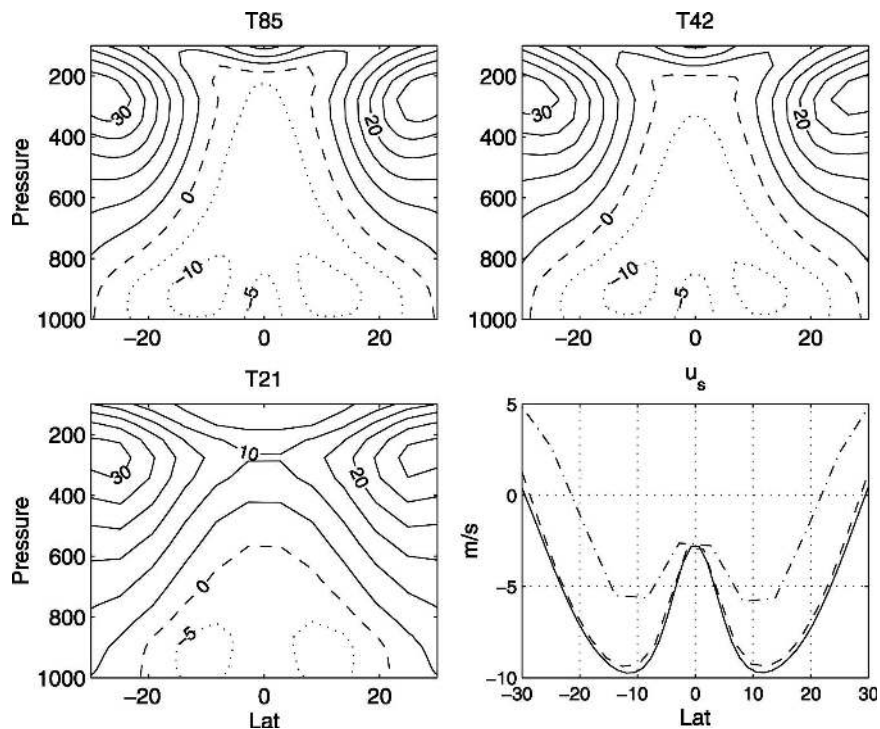

FIG. 9. Zonal winds for the control SBM scheme at (top left) T85, (top right) T42, and (bottom left) T21; and (bottom right) surface zonal winds at T85 (solid), T42 (dashed), and T21 (dashed–dotted).
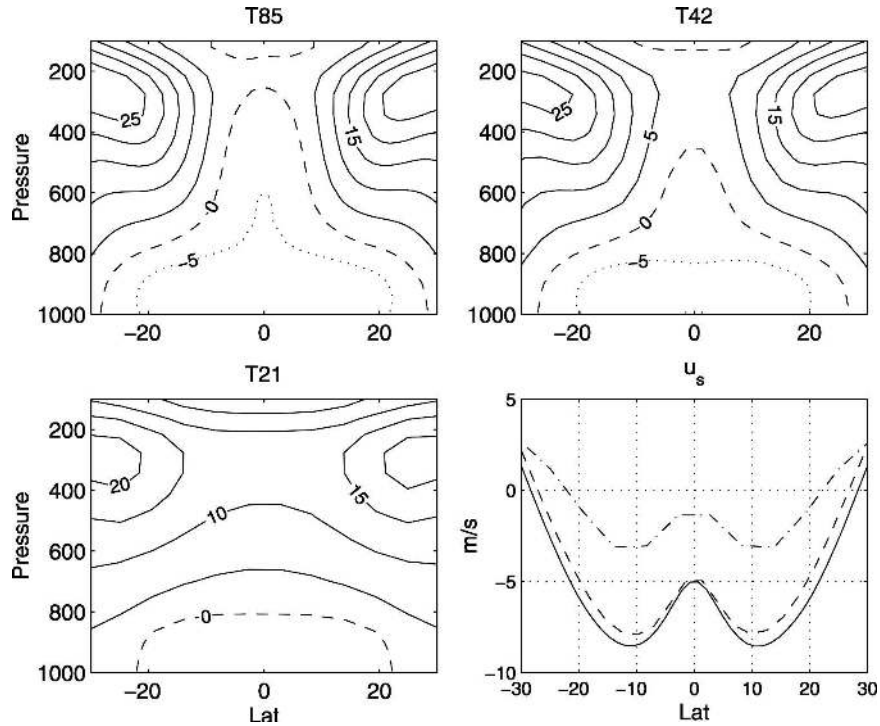
FIG. 10. Zonal winds for the LSC only simulations at (top left) T85, (top right) T42, and (bottom left) T21; and (bottom right) surface zonal winds at T85 (solid), T42 (dashed), and T21 (dashed–dotted).

tion scheme, as in the control case in the above. The tropical precipitation distribution is plotted for $\tau_{\text{SBM}} = 1, 2, 4, 8,$ and 16 h in Fig. 11, and the equatorial precipitation values and maximum Hadley circulation mass transports for these cases are given in Table 3. There is little change in these fields with relaxation times up to 8 h. For instance, the equatorial precipitation values are all within 5%, and the Hadley circulation maxima are within 3% of each other. The $\tau_{\text{SBM}} = 16$ h simulation diverges from the other four simulations however, with sudden increases of 62% in precipitation and 31% in Hadley circulation strength. The Hadley circulation energy transport and gross moist stability are also very similar for the cases up to $\tau_{\text{SBM}} = 8$ h (not shown).

We explain the similarities and differences of the simulations varying relaxation time by first examining the precipitation term [using Eqs. (1) and (3)]:

$$P = \frac{\overline{q} - \overline{q}_{\text{ref}}}{\tau_{\text{SBM}}}, \tag{20}$$

where we use the overbar to denote a vertical integral over the adjusted region; that is, $\overline{\xi} = \int_{p_0}^{p_{\text{LZB}}} \xi \, dp/g$. The expression (20) is exact wherever convective precipitation is occurring since $P = P_q$ using our enthalpy conservation scheme given in Eqs. (5) and (6). Our results show that as τ_{SBM} is varied over a wide range, the precipitation P stays almost constant, therefore pushing the vertical averaged humidity away from the reference profile according to

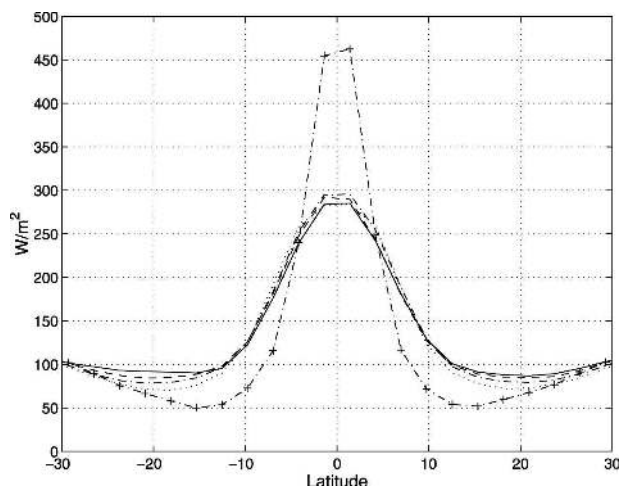$$\overline{q} = \overline{q}_{\text{ref}} + \tau_{\text{SBM}} P. \tag{21}$$

FIG. 11. Precipitation (W m^{-2}) for the SBM scheme with $\tau_{\text{SBM}} = 1$ h (solid), $\tau_{\text{SBM}} = 2$ h (dashed), $\tau_{\text{SBM}} = 4$ h (dashed–dotted), $\tau_{\text{SBM}} = 8$ h (dotted), and $\tau_{\text{SBM}} = 16$ h (dashed–dotted with + symbols), all with RH$_{\text{SBM}} = 0.7$.

TABLE 3. Precipitation at the equator (W m^{-2}) and maximum meridional overturning streamfunction (10^9 kg s^{-1}) for the simulations varying convective relaxation time τ_{SBM}.

Simulation	P(eq)	max(Had)
$\tau_{SBM} = 1$ h	285	182
$\tau_{SBM} = 2$ h	291	184
$\tau_{SBM} = 4$ h	295	186
$\tau_{SBM} = 8$ h	283	185
$\tau_{SBM} = 16$ h	459	242

A similar adjustment of humidity/temperature rather than precipitation occurs in simple models that use Betts–Miller-type convective parameterizations, such as Frierson et al. (2004). We plot the zonal and time mean relative humidity distribution for four of the simulations varying relaxation time in Fig. 12. The relative humidity increases as τ_{SBM} is increased, both within the ITCZ [where Eq. (21) is accurate because convection is occurring most of the time] and in the subtropics (although the changes are less in the subtropics). With the short relaxation time of 1 h, the deep Tropics are kept very close to the reference value of 70% relative

humidity. With $\tau_{SBM} = 8$ h, ITCZ relative humidities exceed 95% in the midtroposphere. The increase in relative humidity in these cases causes slightly more moisture to be advected equatorward by the Hadley circulation, creating less precipitation in the subtropics and more precipitation within the ITCZ with longer relaxation time up to 8 h. This effect is small compared with the precipitation changes in the $\tau_{SBM} = 16$ h simulation however.

With $\tau_{SBM} = 16$ h, the relative humidity is similar to $\tau_{SBM} = 8$ h (not shown). The increase in humidity content described by Eq. (21) cannot hold for arbitrarily high values of the relaxation time because saturation eventually occurs. There is significant large-scale precipitation in the deep Tropics in the 16-h simulation: over 67% of the equatorial precipitation in the 16-h case is large scale, as compared to only 7% large scale for the 8-h case and 0 in the other cases. It is thus not surprising that the $\tau_{SBM} = 16$ h case takes on many of the properties of the LSC only simulations (e.g., increased Hadley circulation and equatorial precipitation). The large change in relative humidity as τ_{SBM} varies over a wide range has little effect on the Hadley
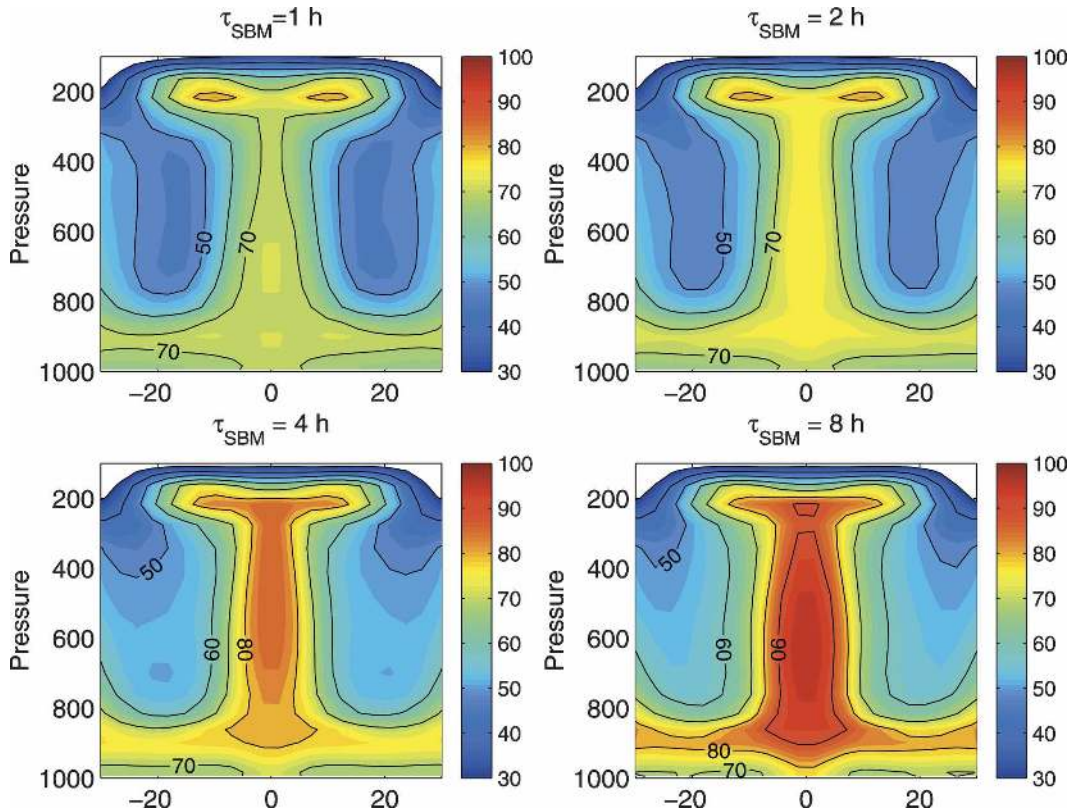

FIG. 12. Relative humidity distribution for (top right) the control SBM scheme, with (top left) $\tau_{SBM} = 1$ h, (bottom left) $\tau_{SBM} = 4$ h, and (bottom right) $\tau_{SBM} = 8$ h.

circulation system unless significant amounts of large-scale condensation can occur. Although the change from the convective-dominated regime to the large-scale-dominated regime happens quickly in parameter space, one can obtain intermediate regimes by tuning the fraction of large scale condensation, which can be increased either by increasing τ_{SBM} or by increasing RH_{SBM} (not shown). For a given set of boundary conditions, virtually any strength of Hadley circulation, precipitation structure, and gross moist stability within the purely convective and purely large-scale limits can be obtained. The study of Held et al. (2007) shows a similar strong sensitivity to the ratio of convective to large-scale precipitation in doubly periodic radiative–convective equilibrium simulations with a full GCM.

The insensitivity of the Hadley circulation and precipitation distribution to convective relaxation time does not mean that all aspects of the tropical circulation are invariant in these simulations. In the study of Frierson (2007), we show that while convectively coupled Kelvin waves dominate the variability of the Tropics in simulations with short relaxation time (e.g., with $\tau_{SBM} = 2$ h), these waves are completely eliminated with higher values of the relaxation time (e.g., with $\tau_{SBM} = 8$ h). Combined with the results of this section, this gives the comforting result that the Hadley circulation system in this model is insensitive to equatorial wave dynamics. This is likely because the eastward-propagating, equatorially confined Kelvin waves primarily propagate energy and moisture in the zonal direction.

A few comments are necessary to compare the results of this section with the study of Fang and Tung (1997). These authors vary the thermal relaxation time for Newtonian cooling in an axisymmetric model and find a large sensitivity of the Hadley circulation to this parameter. With the Newtonian cooling parameterization, the heating rate is proportional to $1/\tau$, assuming a temperature structure consistent with angular momentum conservation within the cell. Therefore, a significantly stronger Hadley circulation is required to transport enough heat to flatten temperatures as the Newtonian relaxation time is decreased. By contrast, changing the convective relaxation time in our model changes the heating only minimally, and no additional meridional fluxes are required to keep the temperatures/zonal winds the same.

A value of $\tau_{SBM} = 16$ h is suggested by the observations of Bretherton et al. (2004); using this with $RH_{SBM} = 0.7$ is ineffective in preventing large-scale condensation from occurring. However, we have found that this relaxation time can be used without large-scale

condensation occurring provided $RH_{SBM} \leq 0.5$ (not shown).

b. Sensitivity to RH_{SBM}

We next study the sensitivity to RH_{SBM}, the relative humidity of the reference profile to which we relax. A first aspect of this dependence we consider is the relative humidity distribution, plotted in Fig. 13 for $\tau_{SBM} = 2$ h and $RH_{SBM} = 0.8$, 0.7, 0.6, and 0.5. The ITCZ humidity is fixed at a slightly larger value than RH_{SBM} in each case, as discussed in the previous section and with Eq. (21). The subtropical humidity varies as well with this parameter, although somewhat less than the ITCZ values: the minimum at 560 hPa varies from 54% in the $RH_{SBM} = 0.8$ case to 38% in the $RH_{SBM} = 0.5$ case.

The evaporation and precipitation distributions in the Tropics are given in Fig. 14. The evaporation increases with decreased relative humidity, but not nearly as much as would be expected from a $1 - RH_{SBM}$ scaling for this quantity. The jump in temperature between the surface and the lowest model level decreases with decreasing RH_{SBM} to oppose the relative humidity change. The evaporation thus increases by only 20% at the equator from the $RH_{SBM} = 0.8$ case to the $RH_{SBM} = 0.5$ case.

The changes in precipitation in Fig. 14 are more complicated. In the subtropics, the precipitation increases uniformly with decreasing RH_{SBM}, along with the evaporation. However, at the equator the changes in precipitation are nonuniform. Part of the reason for this complexity is that while the evaporation increases with decreasing RH_{SBM}, the moisture content of the atmosphere decreases. The Hadley circulation thus converges less moisture toward the equator with the same amount of mass flux. The precipitation in the Tropics is determined by the sum of the evaporation, Hadley cell moisture transport, and eddy moisture fluxes (which each change in these simulations). Changes in the latitudinal structure of these three quantities lead to changes in the structure of the precipitation; for instance the ITCZ is less peaked in the $RH_{SBM} = 0.6$ case. The Hadley circulation mass flux is less sensitive than the precipitation distribution, with maximum values all within 8% (Table 4).

Although the Tropics are more sensitive to the RH_{SBM} parameter than to the τ_{SBM} parameter due to its effect on the evaporation distribution and the moisture fluxes, we emphasize the relative insensitivity to this parameter as well. The insensitivity to RH_{SBM} is especially evident when compared with the changes due to increasing the amount of large-scale condensation, or removing the shallow convection scheme, such as in Fig. 5. The results from this section reinforce the inter-
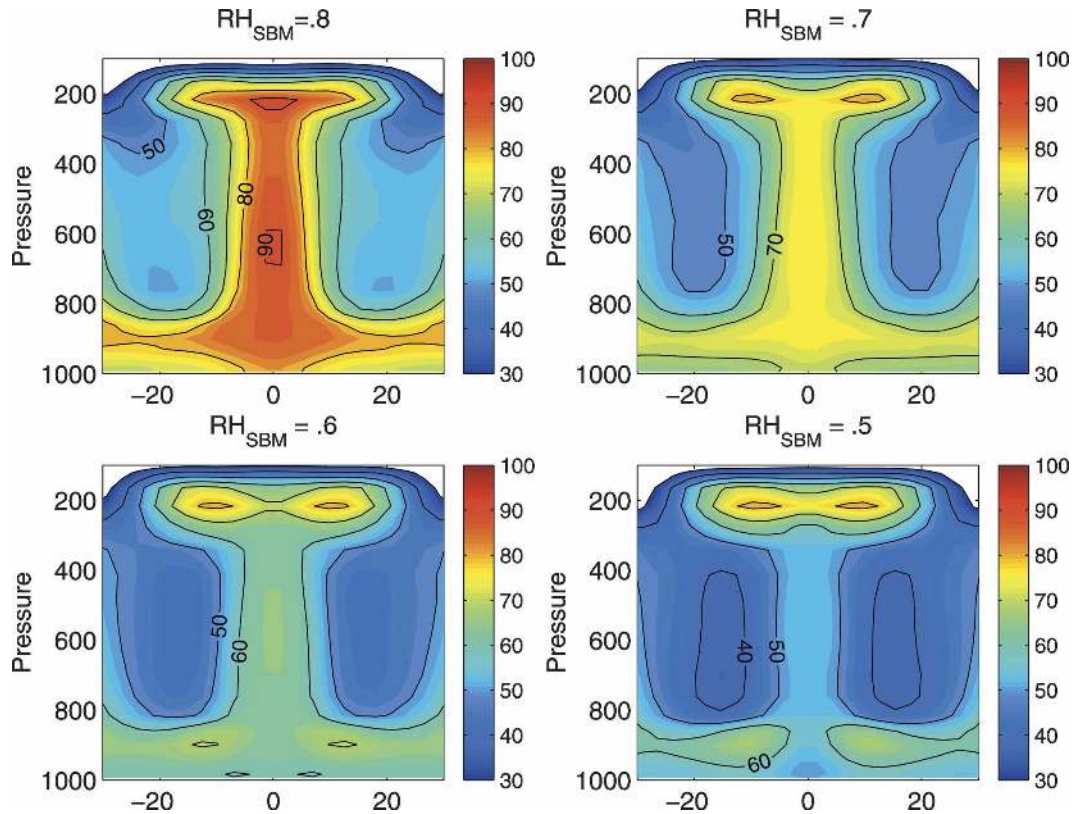
FIG. 13. Relative humidity distribution for (top right) the control SBM scheme, with (top left) $RH_{SBM} = 0.8$, (bottom left) $RH_{SBM} = 0.6$, and (bottom right) $RH_{SBM} = 0.5$.

pretations given in section 3c, that the primary aspect of convection schemes to which the tropical circulation is sensitive is the abruptness of the convective criterion.

5. Discussion and conclusions

In this paper, we have developed a simplification of the convection scheme of Betts and Miller (Betts 1986; Betts and Miller 1986) and studied the response of the tropical circulation to this within an idealized GCM. We have designed the convection scheme to be mathematically continuous when possible, and to have a small amount of tunable parameters, for simplicity and reproducibility of results. Our scheme differs from the standard Betts–Miller scheme in several aspects: first, the reference profiles to which we relax are simplified, removing reference to freezing levels and simplifying the humidity reference profile to a fixed relative humidity from empirically based saturation pressure departures. Additionally, when we switch to the shallow convection scheme, this is now performed in a mathematically continuous manner rather than switching to a specified shallow convection depth. We hope that these simplifications, while losing fidelity with observa-

tions of the current climate, will allow for better simulation of the climate over wide parameter ranges. For instance, we have recently used the SBM scheme in a study of the dynamics of Titan's methane clouds
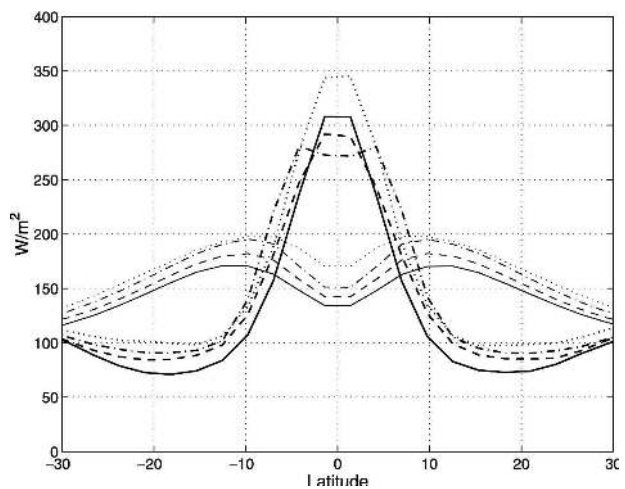

FIG. 14. Precipitation (thick) and evaporation (thin) for the SBM scheme (W m^{-2}) with $RH_{SBM} = 0.8$ (solid), $RH_{SBM} = 0.7$ (dashed), $RH_{SBM} = 0.6$ (dashed–dotted), and $RH_{SBM} = 0.5$ (dotted), all with $\tau_{SBM} = 2$ h.

TABLE 4. Precipitation at the equator (W m^{-2}) and maximum meridional overturning streamfunction (10^9 kg s^{-1}) for the simulations varying the convection scheme RH parameter RH$_{SBM}$.

Simulation	P(eq)	max(Had)
RH$_{SBM}$ = 0.8	308	192
RH$_{SBM}$ = 0.7	291	184
RH$_{SBM}$ = 0.6	272	199
RH$_{SBM}$ = 0.5	345	192

(Mitchell et al. 2006). In this paper, the model of Frierson et al. (2006) with the SBM convection scheme serves an effective intermediate complexity context in which to evaluate the importance of moisture on the tropical general circulation.

We show in this study that the parameterization of moist convection can have a significant effect on the zonally averaged tropical circulation, and we classify some of the aspects of the schemes that cause the differences. The simulations in this study largely fall into two categories. Schemes with an abrupt convective criterion, such as LSC or MCA, which each require saturation of the grid box to precipitate, have significantly different behavior than schemes that are less abrupt. The abrupt-trigger schemes tend to have convective events concentrated near the grid scale, exhibit sensitivity to resolution in fields such as tropical tropospheric zonal wind, and Hadley circulation energy flux, and have a stronger Hadley circulation and larger equatorial precipitation. These properties are consistent with full GCM studies that utilize the MCA convection scheme, such as Manabe et al. (1970, 1974). The parameterization of shallow convection is important as well: the SBM schemes without shallow convection are generally intermediate between the LSC and MCA cases and the smoother SBM simulations with shallow convection.

The gross moist stability is negative in the deep Tropics for the LSC and MCA simulations, implying the tropical atmosphere is kept in a state of convective instability, and even an extremely strong Hadley circulation cannot transport heat poleward. Eddies carry large amounts of latent heat poleward in this case. The addition of the SBM scheme provides a stabilizing influence over the Tropics, allowing the Hadley circulation to transport heat poleward with a more modest circulation.

An alternate interpretation for the reduced Hadley circulation in the SBM schemes with shallow convection is found by examining the energy budget in the subtropics. In this relatively dry region, the atmosphere rarely achieves the saturation necessary to precipitate

with the LSC or MCA schemes. With the SBM schemes, it is easier to convect in the subtropics, and more of the radiative cooling is offset by latent heating, requiring less subsidence to balance energetically. The Hadley circulation is thus reduced in the SBM schemes.

Experiments varying the convective relaxation time show that the zonally averaged circulation is remarkably insensitive to this parameter, as long as the relaxation time is kept sufficiently short to assure that large-scale condensation does not occur. The primary difference in the simulations varying relaxation time is that the relative humidity increases as the relaxation time is lengthened. This adjustment occurs as to keep the latent heating similar for all cases, so the Hadley circulation and precipitation distribution are not affected. The convective relaxation time has a large effect on such aspects of the tropical atmosphere as the intraseasonal variability and the steadiness of convection, which we study in Frierson (2007).

The Tropics are relatively insensitive to the relative humidity parameter RH$_{SBM}$. The ITCZ precipitation changes that are seen as this parameter is varied are nonuniform. The sensitivity of precipitation to RH$_{SBM}$ is largely complicated by the opposing effects of increases in evaporation, and decreases in Hadley circulation moisture transports due to decreased atmospheric moisture content.

To apply these results to the atmosphere or full GCM simulations, it is important to consider the possible effects of the various idealizations made in our physical parameterizations. For instance, the gray radiation scheme has more pronounced radiative cooling in the midtroposphere than in reality, which may influence the structure of the Hadley circulation and the precipitation distribution, as well the importance of shallow convection. Clearly, the lack of clouds in this model could have a wide range of effects on tropical circulations, and while there are analogs to our convection scheme parameters in full GCMs, most full GCM convection schemes are significantly more complex than our SBM scheme. Experiments with full GCM physical parameterizations are necessary to validate the results of this study.

Despite our idealizations, it is quite possible that the theoretical framework we have developed here can be applied to full GCM simulations. Similar large sensitivities to the ratio between convective and large-scale precipitation have been observed using the GFDL AM2 full GCM in simplified geometries (Held et al. 2007). As in this work, the transition between convective- and large-scale-dominated regimes happens quickly in parameter space, and is accompanied by large changes in the climate. While this requires further testing, the

Held et al. (2007) study indicates that our results may be directly applicable to more complex models. It is further interesting to note that while full GCM simulations with the MCA scheme or with a larger fraction of large-scale precipitation often have an unrealistically strong Hadley circulation and a poorer mean climate in general, there are some aspects of the tropical circulation that improve with increased large scale condensation, including the intensity of tropical variability and the speed of tropical waves, which we examine in Frierson (2007). This intermediate complexity model provides a useful realm for understanding the reasons for this behavior, and we hope that this understanding can eventually be transformed into improvements in GCM parameterizations.

Our future course of study with this model on the more realistic end will include the addition of full GCM physical parameterizations of radiation, clouds, and convection to better understand the importance of these feedbacks on our results. On the theoretical end, we are planning a study of the precipitation distribution as moisture content and temperature are varied in an idealized Walker cell domain. We hope this study can better quantify some of the ideas presented in section 3c without the complications of rotation: for instance, the determination and importance of the gross moist stability, eddy moisture fluxes, and subsidence in the dry regions. We then hope to apply these findings back to the problem of the Hadley circulation, with the ultimate goal being a better understanding of the interactions between tropical circulations and moisture over a wide range of climates. rate representation in the stratosphere.

REFERENCES

Arakawa, A., 2004: The cumulus parameterization problem: Past, present, and future. *J. Climate,* **17,** 2493–2525.

Betts, A. K., 1986: A new convective adjustment scheme. Part I: Observational and theoretical basis. *Quart. J. Roy. Meteor. Soc.,* **112,** 677–692.

——, and M. J. Miller, 1986: A new convective adjustment scheme. Part II: Single column tests using GATE wave, BOMEX, and arctic air-mass data sets. *Quart. J. Roy. Meteor. Soc.,* **112,** 693–709.

Bretherton, C., M. E. Peters, and L. E. Back, 2004: Relationships between water vapor path and precipitation over the tropical oceans. *J. Climate,* **17,** 1517–1528.

Brown, R. G., and C. S. Bretherton, 1997: A test of the strict quasi-equilibrium theory on long time and space scales. *J. Atmos. Sci.,* **54,** 624–638.

Chao, W. C., 2000: Multiple quasi equilibria of the ITCZ and the origin of monsoon onset. *J. Atmos. Sci.,* **57,** 641–651.

——, and B. Chen, 2001: Multiple quasi equilibria of the ITCZ and the origin of monsoon onset. Part II: Rotational ITCZ attractors. *J. Atmos. Sci.,* **58,** 2820–2831.

——, and ——, 2004: Single and double ITCZ in an aqua-planet model with constant sea surface temperature and solar angle. *Climate Dyn.,* **22,** 447–459.

Donner, L. J., and V. T. Phillips, 2003: Boundary layer control on convective available potential energy: Implications for cumulus parameterization. *J. Geophys. Res.,* **108,** 4701, doi:10.1029/2003JD003773.

Fang, M., and K. K. Tung, 1997: The dependence of the Hadley circulation on the thermal relaxation time. *J. Atmos. Sci.,* **54,** 1379–1384.

Frierson, D. M. W., 2007: Convectively coupled Kelvin waves in an idealized moist general circulation model. *J. Atmos. Sci.,* **64,** 2076–2090.

——, A. J. Majda, and O. M. Pauluis, 2004: Large scale dynamics of precipitation fronts in the tropical atmosphere: A novel relaxation limit. *J. Commun. Math. Sci.,* **2,** 591–626.

——, I. M. Held, and P. Zurita-Gotor, 2006: A gray-radiation aquaplanet moist GCM. Part I: Static stability and eddy scale. *J. Atmos. Sci.,* **63,** 2548–2566.

——, ——, and ——, 2007: A gray-radiation aquaplanet moist GCM. Part II: Energy transports in altered climates. *J. Atmos. Sci.,* **64,** 1680–1693.

Garner, S. T., D. M. W. Frierson, I. M. Held, O. M. Pauluis, and G. K. Vallis, 2007: Resolving convection in a global hypohydrostatic model. *J. Atmos. Sci.,* **64,** 2061–2075.

Held, I. M., and A. Y. Hou, 1980: Nonlinear axially symmetric circulations in a nearly inviscid atmosphere. *J. Atmos. Sci.,* **37,** 515–533.

——, M. Zhao, and B. Wyman, 2007: Radiative radiative–convective equilibrium using GCM column physics. *J. Atmos. Sci.,* **64,** 228–238.

Hess, P. G., D. S. Battisti, and P. J. Rasch, 1993: Maintenance of the intertropical convergence zones and the large-scale tropical circulation on a water-covered earth. *J. Atmos. Sci.,* **50,** 691–713.

Janjic, Z. I., 1994: The step-mountain Eta coordinate model: Further developments of the convection, viscous sublayer, and turbulence closure schemes. *Mon. Wea. Rev.,* **122,** 927–945.

Manabe, S., J. L. Holloway Jr., and H. M. Stone, 1970: Tropical circulation in a time-integration of a global model of the atmosphere. *J. Atmos. Sci.,* **27,** 580–612.

——, D. G. Hahn, and J. L. Holloway Jr., 1974: The seasonal variation of the tropical circulation as simulated by a global model of the atmosphere. *J. Atmos. Sci.,* **31,** 43–83.

Mechoso, C. R., and Coauthors, 1995: The seasonal cycle over the tropical Pacific in coupled ocean–atmosphere general circulation models. *Mon. Wea. Rev.,* **123,** 2825–2838.

Mitchell, J. L., R. T. Pierrehumbert, D. M. W. Frierson, and R. Caballero, 2006: The dynamics behind Titan's methane clouds. *Proc. Natl. Acad. Sci.,* **103,** 18 421–18 426.

Moorthi, S., and M. J. Suarez, 1992: Relaxed Arakawa–Schubert: A parameterization of moist convection for general circulation models. *Mon. Wea. Rev.,* **120,** 978–1002.

Neelin, J. D., and I. M. Held, 1987: Modeling tropical convergence based on the moist static energy budget. *Mon. Wea. Rev.,* **115,** 3–12.

——, and J. Yu, 1994: Modes of tropical variability under convective adjustment and the Madden–Julian oscillation. Part I: Analytical theory. *J. Atmos. Sci.,* **51,** 1876–1894.

——, and N. Zeng, 2000: A quasi-equilibrium tropical circulation model—formulation. *J. Atmos. Sci.,* **57,** 1741–1766.

Numaguti, A., 1993: Dynamics and energy balance of the Hadley circulation and tropical precipitation zones. Part I: Significance of the distribution of evaporation. *J. Atmos. Sci.,* **50,** 1874–1887.

——, 1995: Dynamics and energy balance of the Hadley circulation and tropical precipitation zones. Part II: Sensitivity to meridional SST distribution. *J. Atmos. Sci.,* **52,** 1128–1141.

Satoh, M., 1994: Hadley circulations in radiative–convective equilibrium in an axially symmetric atmosphere. *J. Atmos. Sci.,* **51,** 1947–1968.

Sobel, A. H., J. Nilsson, and L. M. Polvani, 2001: The weak temperature gradient approximation and balanced tropical moisture waves. *J. Atmos. Sci.,* **58,** 3650–3665.

Yu, J., and J. Neelin, 1994: Modes of tropical variability under convective adjustment and the Madden–Julian oscillation. Part II: Numerical results. *J. Atmos. Sci.,* **51,** 1895–1914.

——, and ——, 1997: Analytic approximations for moist convectively adjusted regions. *J. Atmos. Sci.,* **54,** 1054–1063.

Zhang, G. J., 2002: Convective quasi-equilibrium in midlatitude continental environment and its effect on convective parameterization. *J. Geophys. Res.,* **107,** 4220, doi:10.1029/2001JD001005.

——, 2003: Convective quasi-equilibrium in the tropical western Pacific: Comparison with midlatitude continental environment. *J. Geophys. Res.,* **108,** 4592, doi:10.1029/2003JD003520.